

## Theoretical line strengths for the $4d^{10}1S - 4d^94f^1P^0$ resonance transition in the palladium isoelectronic sequence

S. M. Younger

National Measurement Laboratory, National Bureau of Standards, Washington, D. C. 20234

(Received 5 June 1980)

Theoretical line strengths for the  $4d^{10}1S - 4d^94f^1P^0$  resonance transition in the palladium isoelectronic sequence have been computed in three approximations: configuration-averaged Hartree-Fock, term-dependent Hartree-Fock, and many-body perturbation theory. The Hartree-Fock  $4f$  state exhibits pronounced term dependence in the intermediate ionization stages III-XV, with the configuration-averaged radial orbital collapsing more rapidly with  $Z$  than the  $4f^1P^0$  term-dependent orbital due to the large repulsive exchange interaction with the  $4d^9$  subshell in the latter. The  $4d-4f$  oscillator strength is small for low ionization stages, and does not reach a maximum until Ba XI. Contracted orbital many-body perturbation theory calculations confirm that, as expected for this closed-shell ground-state system, most of the correlation effects are concentrated in the  $4d^94f^21S$  configuration mixing with the ground state. As a comparison, Hartree-Fock data are also given for the transition  $4d^{10}1S - 4d^95p^1P^0$ . For  $Z < 60$  the  $5p^1P^0$  state is the lowest-lying  $1P^0$  in the Pd I sequence.

### I. INTRODUCTION

Although there exist many theoretical and experimental studies of transition probabilities in atoms and ions lighter and with fewer electrons than iron,<sup>1</sup> few very heavy isoelectronic sequences have so far been systematically explored. Several calculations<sup>2,3</sup> have been performed on the single-valence-electron Cu sequence, and Fischer and Hansen,<sup>4</sup> Shorer,<sup>5</sup> and Weiss<sup>6</sup> have studied neighboring Zn-like ions. There are several reasons why it is important to continue this effort toward even heavier isoelectronic sequences with more complex structure. Data on heavy highly ionized atoms are required for modeling and diagnostics purposes in high-temperature plasma research relating to the fusion effort. Also, calculations on moderately heavy isoelectronic sequences have indicated that several new and interesting effects are to be observed in the structure of heavy ions, such as the term dependence of the radial wave functions and the crossing of energy levels along an isoelectronic sequence.

We have chosen the palladium isoelectronic sequence for such a study, since it is a heavy sequence with a relatively simple excitation spectrum ( $4d^{10}1S$  ground state) compared with most other heavy ions. The resonance transition  $4d^{10}1S - 4d^94f^1P^0$  is expected to be quite strong due to the large overlap between the  $4d$  and  $4f$  orbitals, and might be observable in highly ionized atoms such as Xe XI and WXXIX occurring in high-temperature plasmas. The Pd I sequence might also serve as a testing ground for new and more accurate methods for the correction of cascade errors occurring in beam-foil measurements of excited-state lifetimes.<sup>7</sup>

Since the optical electrons involved in the present study have orbital angular momenta of 2 and 3,

relativistic effects on the line strengths are expected to be smaller than in the neighboring iron sequence, where the deeply penetrating  $5s$  orbital sees a potential substantially different from the nonrelativistic Hartree-Fock calculation.<sup>8,9</sup>

In order to map out the general behavior of the energy levels and nonrelativistic line strengths along the palladium sequence, Hartree-Fock calculations, both configuration-averaged and term-dependent, were made for a number of ions up to U XLVII. Using data from these calculations, a simple perturbation-theory correction was applied to the ground state to obtain partially correlated line strengths. In order to evaluate the effectiveness of this simple correction, many-body perturbation-theory calculations including all excited configurations contributing to the first-order line-strength correction were performed for Xe IX, Nd XV, and WXXIX.

In addition, Hartree-Fock calculations were done for the  $4d^{10}1S - 4d^95p^1P^0$  transition in selected ions.

Section II presents the results of the Hartree-Fock calculations for the  $4d-4f$  transition. Section III describes the perturbation calculations, including a brief summary of the contracted orbital many-body perturbation theory (COMBPT) method. Section IV summarizes the calculations.

### II. HARTREE-FOCK CALCULATIONS FOR THE $4d^{10}1S - 4d^94f^1P^0$ TRANSITION

#### A. Energy levels

Hartree-Fock calculations were performed for a number of ions in the palladium isoelectronic sequence with charge states up to 46 (U XLVII) using a version of Fischer's multiconfiguration Hartree-Fock code.<sup>10</sup> To assess the term dependence of the excited state, parallel calculations were executed using the configuration-averaged potential

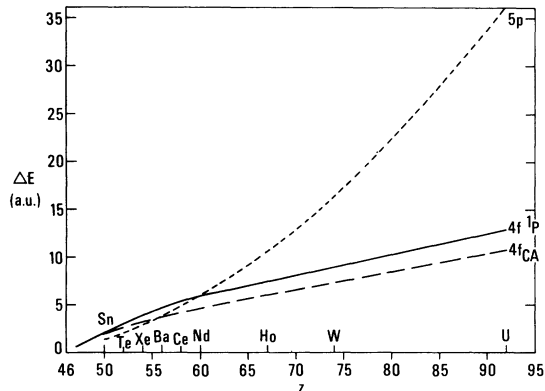


FIG. 1. Nonrelativistic Hartree-Fock energies of the  $4d^9 4f_{CA}$ ,  $4d^9 4f_{1P}$ , and  $4d^9 5p_{CA}$  configurations relative to the ground state (atomic units).

(sometimes called the center-of-gravity potential) derived from the average energy of the  $4d^9 4f$  configuration<sup>11</sup> and the correct term-dependent potential for the  $^1P$  level. The total energy of the  $^1P$  term is related to the configuration-averaged energy  $E_{CA}$  by

$$E(4d^9 4f^1 P) = E_{CA}(4d^9 4f) - 0.22857 F^2(df) - 0.09524 F^4(df) + 1.95714 G^1(df) - 0.019051 G^3(df) - 0.021645 G^5(df). \quad (1)$$

Note the large positive coefficient for the  $G^1(df)$  term. The total energies of the triplets  $^3P$  and  $^3D$  are close to the configuration-averaged value.

The  $Z$  dependence of the  $4f_{CA}$  and  $4f_{1P}$  energy levels, as well as the nonrelativistic configuration-averaged energy of the  $4d^9 5p$  configuration, is illustrated in Fig. 1. The  $4d^9 5p$  configuration is the first excited state until Ba XI, when it crosses the  $4d^9 4f$  triplets. Note that  $4d^9 5p$  remains the

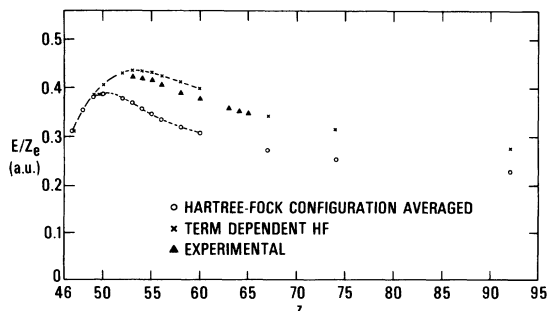


FIG. 2. Nonrelativistic Hartree-Fock  $4d^{10} - 4d^9 4f_{1P}$  excitation energy scaled by the effective nuclear charge  $Z_e = Z - 45$ .  $\blacktriangle$ , experimental (Ref. 13).

TABLE I. Hartree-Fock  $4d^{10} - 4d^9 4f$  excitation energies for Pd I isoelectronic ions (atomic units).

Ion	$\Delta E(4d^{10} - 4d^9 4f)$		
	CA	$^1P$	$E(\text{expt})$
Ag II	0.6242	0.6267	
Cd III	1.060	1.064	
In IV	1.516	1.541	
Sn V	1.937	2.024	
Te VII	2.643	3.010	
I VIII	2.934	3.484	3.392 9 <sup>a</sup>
Xe IX	3.210	3.906	
Cs X	3.464	4.313	4.157 71 <sup>b</sup>
Ba XI	3.704	4.668	4.493 62 <sup>b</sup>
Ce XIII	4.141	5.273	5.105 5 <sup>b</sup>
Nd XV	4.584	5.944	5.660 1 <sup>b</sup>
Ho XXII	6.007	7.539	
W XXXIX	7.347	9.098	

<sup>a</sup> Reference 13.

<sup>b</sup> Reference 12.

lowest  $^1P^0$  configuration accessible to the ground state via electric dipole transitions until Nd XV.

An expanded plot of the  $4f$  energy relative to the ground state is given in Fig. 2, where the transition energies are scaled by the effective charge. Although the CA and  $^1P$  energies are in good agreement at low ionization stages, for  $Z > 50$  a rapid divergence sets in which persists through the high- $Z$  end of the graph. This behavior reflects the collapse of the  $4f$  orbital which occurs at Sn V ( $Z = 50$ ) for the CA case, but not until about  $Z = 58$  for the  $^1P$  function, due to the influence of the large repulsive exchange potential between the  $4d^9$  core and the  $4f$  electron. Table I gives numerical values for the  $4f$  energies.

The collapse of the  $4f$  radial wave function along the isoelectronic sequence is illustrated in Fig. 3,

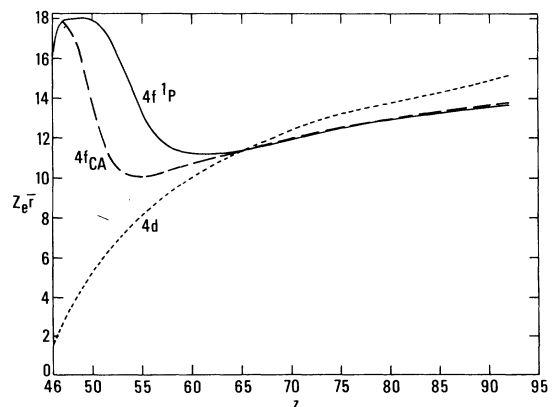


FIG. 3. Mean radii of the  $4d_{1s}$ ,  $4f_{CA}$ , and  $4f_{1P}$  Hartree-Fock orbitals scaled by the effective nuclear charge  $Z_e = Z - 45$ .

which plots the scaled mean radii of the  $4f_{CA}$  and  $4f_{1P}$  orbitals, as well as that of the  $4d^{10}$  ground state vs the nuclear charge. The  $4f_{CA}$  function undergoes a rapid collapse starting at the neutral end of the sequence, finishing at XeIX. The  $4f_{1P}$  orbital is essentially hydrogenic until TeVII when a gradual collapse begins. The  $4f_{1P}$  orbital is not fully collapsed until after Nd XV. Note that at high  $Z$  the mean radii of the  $4f$  states are less than that of the  $4d$  ground state, as one would expect from the asymptotic behavior of  $\bar{r}$ .

Plots of the  $4d_{1S}$ ,  $4f_{CA}$ , and  $4f_{1P}$  radial orbitals for AgII, SnV, TeVII, XeIX, Nd XV, and W XXIX are shown in Fig. 4. In AgII both  $4f$  functions are very close to hydrogenic orbitals with  $Z=2$ . As the nuclear charge increases, the mean radii of the  $4f$  state decreases with respect to the  $4d$ , causing a more complex interaction with the many-electron core. One then finds deviations from a hydrogen-like orbital in both functions, with the collapse of the  $4f_{1P}$  function being retarded by the presence of the large exchange term involving the

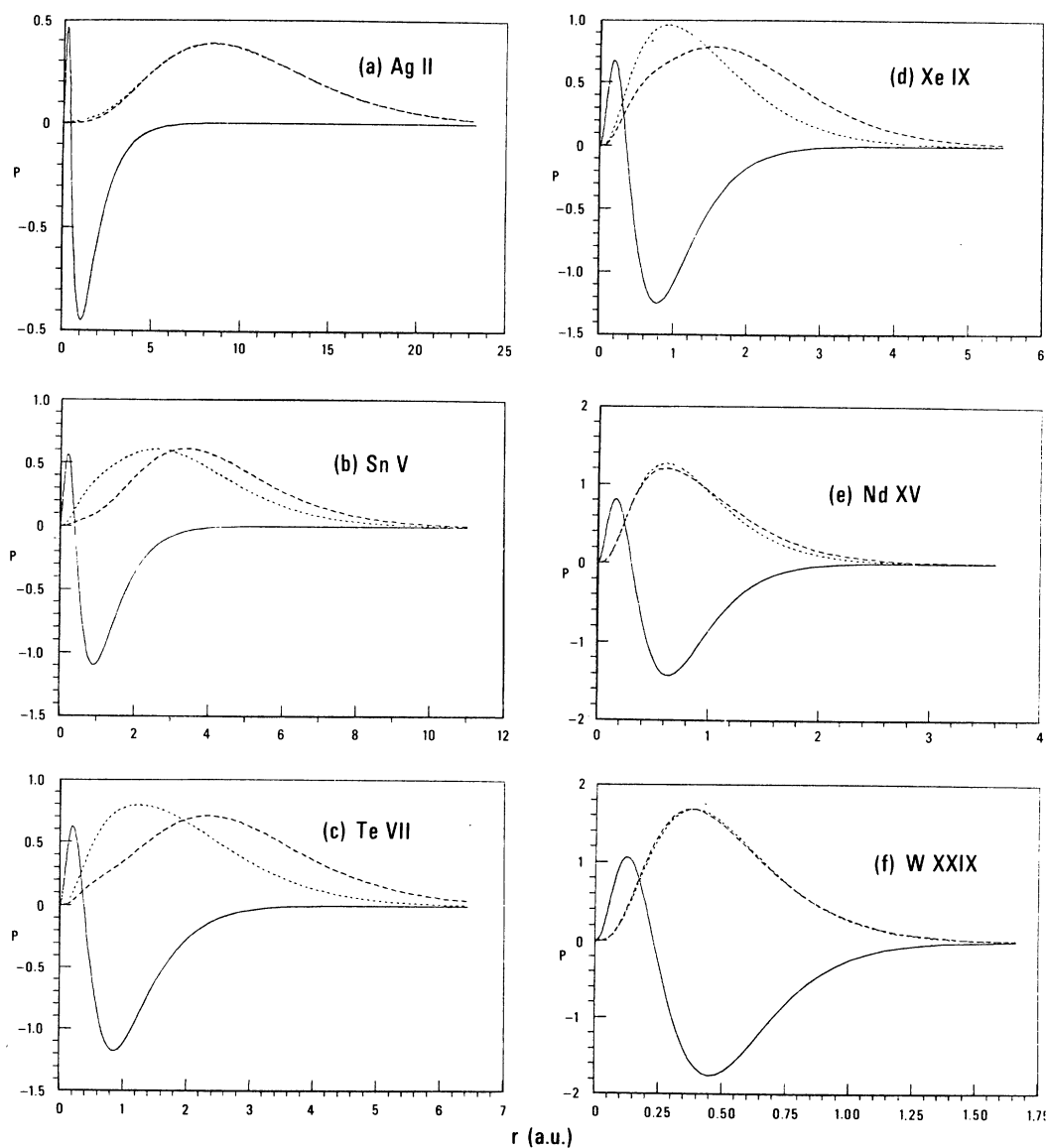


FIG. 4. Hartree-Fock  $4d_{1S}$  (solid),  $4f_{CA}$  (dashed), and  $4f_{1P}$  (dotted) radial orbitals. At AgII the  $4f$  functions are essentially hydrogenlike. As the nuclear charge increases the  $4f_{CA}$  orbital undergoes a rapid collapse with respect to the  $4d_{1S}$ . The large exchange repulsion term in the  $4f_{1P}$  wave equation delays the collapse of that orbital until much higher charge states. Note the distortion of the  $4f_{1P}$  orbital near the nucleus.

$4d$  subshell. Careful examination of Fig. 4 shows that the  $4f_{1p}$  function is deformed near the nucleus, reflecting a modification of the effective potential experienced by the  $4f$  orbital in the vicinity of the  $4d$  subshell due to the large  $df$  exchange integral. The term dependence of the  $4f$  radial orbital is greatest at TeVII, after which the nuclear potential begins to dominate the details of the inter-electronic interaction. By Ho XXIX the  $4f_{CA}$  and  $4f_{1p}$  functions are virtually identical.

The Hartree-Fock  $4f_{1p}$  energies are in reasonably good agreement with the observations of Sugar<sup>12</sup> for Cs through Nd, and of Even-Zohar and Fraenkel<sup>13</sup> for I VIII. The experimental excitation energies are only about 4% lower than the term-dependent Hartree-Fock values, a surprising result in view of the many-body character of the system.

### B. Line strengths and oscillator strengths

The line strength  $S$  for a  $d^{10}1S - d^9f^1P$  transition in the single configuration approximation is<sup>11</sup>

$$S = |\langle \Psi_{4d^{10}} | r | \Psi_{4d^9f^1} \rangle|^2 \\ = 6 \left| \int_0^\infty P_{4d}(r) r P_{4f}(r) dr \right|^2, \quad (2)$$

where  $P_i$  is a radial orbital and  $\Psi$  a total wave function. Overlap terms between orbitals not undergoing a transition are assumed to be unity. The oscillator strength is then  $f = \frac{2}{3} \Delta E S$  where  $\Delta E$  is the transition energy in atomic units.

The different rates of collapse with increasing nuclear charge of the  $4f_{CA}$  and  $4f_{1p}$  radial functions result in radically different line and oscillator strengths associated with those orbitals. Table II gives the line strength computed for the  $4d^{10}1S - 4d^94f^1P$  transition using  $4f$  orbitals from the configuration-averaged and term-dependent Hartree-Fock approximations. Figure 5 shows a plot of the corresponding oscillator strengths, computed from the line strengths of Table II and observed or extrapolated transition energies. Certainly at the high- $Z$  end of the sequence such an energy extrapolation is far from accurate due to large relativistic effects; we have plotted the  $f$  value in this region only to map the nonrelativistic systematic trend.

The hydrogenic character of the  $4f$  orbitals at low- $Z$  results in a small oscillator strength for the first few ions. The rapidly collapsing  $4f_{CA}$  function causes a rapid rise in the configuration-averaged oscillator strength, the curve reaching a maximum at Xe IX. The  $4f_{1p}$  oscillator strength does not peak until Ba XI. Note that at Sn V the two curves differ by more than 250%.

TABLE II. Hartree-Fock line strengths for the  $4d^{10}1S - 4d^94f^1P$  transition in Pd I-like ions.

Ion	$S_{CA}$	$S_{1p}$
Ag II	0.3032	0.2357
Cd III	0.9822	0.5637
In IV	2.276	0.9701
Sn V	3.976	1.445
Te VII	5.252	2.599
I VIII	4.971	3.180
Xe IX	4.556	3.579
Cs X	4.133	3.701
Ba XI	3.744	3.593
Nd XV	2.587	2.606
Ho XXIX	1.533	1.514
W XXIX	1.015	0.9934

### III. PERTURBATION THEORY FOR THE $4d4f$ LINE STRENGTH

#### A. Basis sets

The application of many-body diagrammatic perturbation theory (MBPT) to the calculation of electron correlation effects in atomic transition probabilities has been described elsewhere.<sup>3,14</sup> In the present calculation a variation on the usual technique of generating virtual orbitals for use in evaluating the correlation diagrams is employed, known as "contracted orbital" many-body diagrammatic perturbation theory (COMBPT).<sup>15</sup> In this method the virtual spectrum is restricted to a set of square integrable functions by constructing a potential barrier about the atom. If such a barrier is placed sufficiently far from the nucleus, the occupied states of the system will be left unaffected, but the virtual spectrum will be compressed into a few negative- and positive-energy orbitals which, although still comprising a relatively complete set of functions for the description

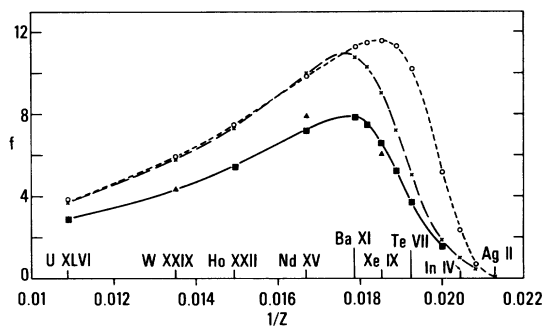


FIG. 5. Oscillator strength of the  $4d^{10}1S - 4d^94f^1P^0$  transition along the Pd I isoelectronic sequence, plotted against  $1/Z$ . Dot,  $4f_{CA}$ ; dash,  $4f_{1p}$ ; ■ solid,  $4f_{1p}$  with  $4f^2$  excitation; ▲  $4f_{1p}$  with all first-order perturbation corrections to the dipole matrix element.

of correlation effects within bound systems, does not have the computer-bound unwieldiness of the large continuum basis sets used in the standard formulation of MBPT. Indeed, such a circumvention has the desirable effect of simulating in a perturbation formalism the rapidly converging basis sets used in multiconfiguration Hartree-Fock and superposition-of-configuration calculations, and has been shown to lead to results of comparable accuracy in calculations of correlation energies of small atoms.<sup>15</sup>

The zeroth-order Hamiltonian  $H_0$  specifies the set of occupied and virtual orbitals for each symmetry which are to be used in the evaluation of the correlation diagrams. For  $l=0, 1$ , and 2 orbitals  $H_0$  was chosen as the Hartree-Fock Hamiltonian for the  $1s^2 2s^2 2p^6 3s^2 3p^6 3d^{10} 4s^2 4p^6 4d^{10} 1S$  closed-shell core:

$$\begin{aligned} \langle a | H_0 (l=0, 1, 2) | b \rangle &= \langle a | T | b \rangle \\ &+ \sum_{i,j}^{46} (\langle ai | v | bj \rangle - \langle ai | v | jb \rangle). \end{aligned} \quad (3)$$

The sum extends over all electrons in the atom up to but not including the  $4f$ . For  $l=3$ ,  $H_0$  was taken as the configuration-averaged Hartree-Fock Hamiltonian for the  $4d^9 4f$  configuration, constructed with occupied bound-state orbitals which were eigenfunctions of Eq. (3)—i. e., the usual Hartree-Fock bound states:

$$\begin{aligned} \langle a | H_0 (l=3) | b \rangle &= \langle a | T | b \rangle \\ &+ \sum_{i,j}^{35} (\langle ai | v | bj \rangle - \langle ai | v | jb \rangle) \\ &+ 9 \langle 4da | v | 4db \rangle - \frac{9}{10} (\dots), \end{aligned} \quad (4)$$

where the ellipsis represents the  $4d^{10} nf$  exchange term,  $T$  is the sum of the kinetic energy and all other single-particle operators, and  $v$  is the Coulomb interaction  $v_{ij} = 1/|r_i - r_j|$ . Virtual states with  $l > 3$  do not appear in the first-order-correlation correction to the dipole matrix element. The occupied states  $1s, 2s, \dots, 4d$  occurring in Eqs. (3) and (4) are Hartree-Fock orbitals from the  $4d^{10} 1S$  ground state of a Pd-like ion. The  $l=3$  potential was chosen to model the  $4d^9 4f_{CA}$  state. Thus the excited state is not a true Hartree-Fock state and single-particle corrections (corresponding to a violation of Brillouin's Law) will occur in the perturbation expansion. In practice, the  $P_{4f}$  from Eq. (4) was found to be almost identical to a true configuration-averaged Hartree-Fock calculation for the  $4d^9 4f$  configuration, the difference being only in the third significant figure of the radial orbital.

## B. Line strengths

Perturbation theory allows one to write the initial- and final-state wave functions as sums of zeroth-order reference states  $\Psi^0$ , and correlation components  $\bar{\chi}$ :

$$\Psi_i = \Psi_i^0 + \bar{\chi}_i, \quad (5)$$

$$\Psi_f = \Psi_f^0 + \bar{\chi}_f. \quad (6)$$

The correlated dipole matrix element is then

$$\begin{aligned} \langle \Psi_i | D | \Psi_f \rangle &= \langle \Psi_i^0 | D | \Psi_f^0 \rangle + \langle \bar{\chi}_i | D | \Psi_f^0 \rangle \\ &+ \langle \Psi_i^0 | D | \bar{\chi}_f \rangle + \langle \bar{\chi}_i | D | \bar{\chi}_f \rangle, \end{aligned} \quad (7)$$

i. e., a sum of the zeroth-order matrix element, two matrix elements involving a zeroth order and a correlation function and one involving two correlation components. The last of these is a second-order effect and is neglected in what follows. For simplicity of notation, we define  $\chi$  as that part of  $\bar{\chi}$  (itself an antisymmetrized wave-function correction analogous to an excited configuration in a superposition of configuration calculation) containing virtual excitations of the bound orbitals.

For the  $4d^{10} 1S$  ground state of a Pd-like ion the first-order correction to the Hartree-Fock wave function involving correlation between a  $4d$  optical electron and another  $n=4$  orbital is

$$\chi_{4d4i} = \sum_{nm} \frac{\langle 4d4i | v | nm \rangle}{\epsilon_{4d} + \epsilon_{4i} - \epsilon_n - \epsilon_m} \phi_n \phi_m, \quad (8)$$

where  $\phi_n$  and  $\phi_m$  are virtual spin orbitals with eigenvalues  $\epsilon_n$  and  $\epsilon_m$ . In the  $4d^9 4f^1 P$  excited state there is a pair correlation function

$$\chi_{4f4i}^{\text{pair}} = \sum_{nm} \frac{\langle 4f4i | v | nm \rangle}{\epsilon_{4f} + \epsilon_{4i} - \epsilon_n - \epsilon_m} \phi_n \phi_m \quad (9)$$

and a single-particle function, which for the  $4f$  orbital is

$$\chi_{4f}^{\text{SP}} = \sum_{n>4} \frac{\langle 4f | \Delta | nf \rangle}{\epsilon_{4f} - \epsilon_{nf}} \phi_{nf}, \quad (10)$$

where  $\Delta$  is defined by

$$\langle 4f | \Delta | nf \rangle = \sum_{i=1}^{46} (\langle 4fi | v | (nf)i \rangle - \langle 4f | V | nf \rangle) \quad (11)$$

with  $V$  the potential in which the  $4f$  orbital was computed. Such single-particle terms arise since the  $4f$  orbital is actually a virtual orbital computed in the  $V^{n-1}$  potential of the ground state. Brillouin's theorem is not satisfied for the  $4f$  virtual orbital. The effect of adding  $\chi_{4f}^{\text{SP}}$  to  $\Psi_f^0$  is to produce a single-particle orbital in close agreement with a true Hartree-Fock  $4f_{1P}$  orbital, as is illustrated in Fig. 6 for XeIX. The coefficients in the perturbation expansion of  $\phi_{4f1P}$  in terms of the basis set derived from Eq. (10) were found to agree well

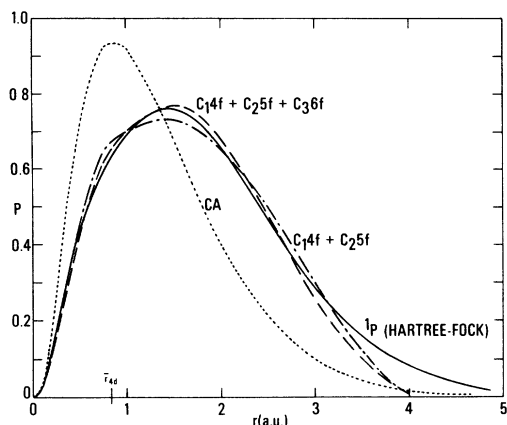


FIG. 6. Correction of the Xe IX  $4f_{CA}$  orbital by first-order single-particle diagrams to produce a single-particle orbital in good agreement with the  $4f_{1p}$  Hartree-Fock orbital. Dot,  $4f_{CA}$ ; dash,  $4f_{CA}$  modified by single-particle wave-function diagrams appearing in first order; solid,  $4f_{1p}$  Hartree-Fock orbital.

with expansion coefficients obtained by numerically fitting the Xe IX  $4f_{1p}$  function with the virtual basis.

The diagrammatic representation of the dipole matrix element is shown in Fig. 7(a). Diagrams corresponding to all nonzero first-order corrections to the dipole matrix element are shown in Figs. 7(b)–7(f). Diagram 7(b) and its exchange 7(c) represent pair correlations in the initial state, 7(d) and 7(e) pair correlation in the final state, and 7(f) single-particle contributions involving the  $4f$  state. The excitation symmetries of the virtual excitations  $k$  which are allowed in each diagram

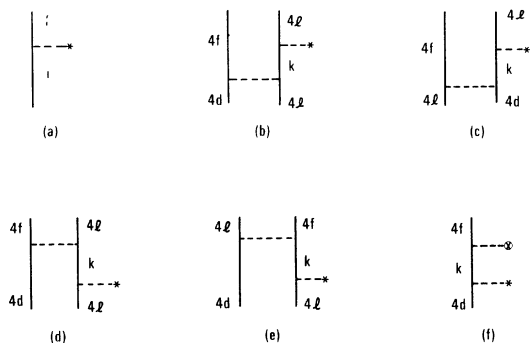


FIG. 7. Perturbation diagrams corresponding to all nonzero first-order corrections to the  $4d$ - $4f$  dipole matrix element. (a) Diagrammatic representation of the dipole matrix element; (b) and (c) pair correlation in the initial state; (d) and (e) pair correlation in the final state; (f) single-particle corrections to the  $4f$  state.  $4l$  represents a nonexcited  $n=4$  core state, i.e.,  $4s$ ,  $4p$ , or  $4d$ .

TABLE III. Perturbation corrections to the  $4d-4f$  dipole matrix element.

Diagram	Xe IX	Nd XV	W XXIX
7(a)	-1.219	-0.9257	-0.5812
7(b)	0.1632	0.1292	0.0786
7(c)	-0.0025	-0.0041	-0.0008
7(d)	0.025	-0.0201	0.0041
7(e)	0.007	-0.0032	-0.0011
7(f)	0.139	-0.0086	0.0000
Total	-0.8873	-0.8325	-0.5004
Hartree-Fock	-1.092	-0.9320	-0.5754
7(a) + 7(f)	-1.080	-0.9343	-0.5812
Initial-state pair	0.161	0.1251	0.0778
Final-state pair	0.032	-0.0233	0.0030
Total	-0.887	-0.8325	-0.5004
$S_{MBPT}$	2.36	2.079	0.7512
$f_{MBPT}$	5.95	7.903	4.381

are limited by the selection rules on the dipole operator. A normalization correction is also required, which is of the form

$$\eta^2 = (1 + \langle \chi_i | \chi_i \rangle)(1 + \langle \chi_f | \chi_f \rangle). \quad (12)$$

Such a correction is necessary since the present formulation of the line strength assumes normalized total wave functions, whereas each orbital appearing in the perturbation basis set is individually unit normalized.

Correlation corrections to the dipole matrix element for several Pd-like ions corresponding to diagrams 7(b)–7(f) are tabulated in Table III, which also gives the resulting line and oscillator strengths.

Since the  $4f_{1p}$  orbital is a mixture of the  $nf$  virtual orbitals, it is necessary to include in Figs. 7(b) and 7(c) diagrams involving excitations to the  $5f$ ,  $6f \dots$  component of the  $4f_{1p}$  orbital. Such contributions were included in Table III.

By far the dominant correction to the Hartree-Fock dipole matrix element involves the ground-state pair excitation  $4d4d' \rightarrow nfmf$ . Over 95% of this correlation correction is concentrated in the excitation  $4d^{10} \rightarrow 4d^8 4f^2$ . Such  $n l^2 \rightarrow n(l+1)^2$  correlation is also observed in other closed-shell systems where the dominant excited configuration is in the ground-state shell, such as Be- and Ar-like ions,<sup>6</sup> and suggests that a good approximation to the full correlation problem may be obtained by retaining only this one excitation. Furthermore, since the  $4f$  virtual orbitals were found to be practically identical to the configuration-averaged Hartree-Fock orbitals, one might apply such a correction using the matrix elements and eigenvalues computed in the course of the Hartree-Fock calculation. A comparison of line strengths com-

TABLE IV.  $4d^{10}1S-4d^94f^1P^0$  line strengths computed in the  $4f^2$ -only approximation compared to the results of the full first order MBPT calculation.

Ion	$S_{HF}$	$S(4f^2 \text{ only})$	$S(\text{Full MBPT})$
Sn v	1.445	1.240	
Te vii	2.599	1.923	
I viii	3.180	2.326	
Xe ix	3.579	2.612	2.36 (2.535) <sup>a</sup>
Cs x	3.701	2.699	
Ba xi	3.593	2.617	
Nd xv	2.606	1.899	2.079 (1.964) <sup>a</sup>
Ho xxii	1.514	1.121	
W xxix	0.9934	0.7466	0.7512 (0.7602) <sup>a</sup>

<sup>a</sup> Numbers in parentheses correspond to initial-state correlation only.

puted using only the  $4d4d' \rightarrow 4f4f'$  Hartree-Fock pair excitation with the results of noncorrelated Hartree-Fock and full first-order perturbation calculations is made in Table IV. For XeIX and NdXV, the deviation between the simple approximation and the full first-order results are on the order of 10% while for WXXIX agreement is almost exact. Note that in XeIX the effect of excited-state correlation and further ground-state correlation beyond  $4f^2$  excitation is to reduce the line strength, while in NdXV the opposite is true.

The effect of higher-order terms in the perturbation expansion for the dipole matrix element was investigated by examining higher-order diagrams containing excitations of the type  $4d4d' \rightarrow 4f4f'$ . It is somewhat surprising that for this many-electron system such higher-order diagrams were found to change the first-order results by less than 1%.

#### IV. DISCUSSION

Figure 5 compares the oscillator strengths for the  $4d^{10}1S-4d^94f^1P$  transition resulting from the approximations described above. The effects of term dependence in the upper state and correlation in the ground state are pronounced and result in a value substantially less than the Hartree-Fock configuration-averaged value.

Relativistic effects on the  $4d-4f$  line strength

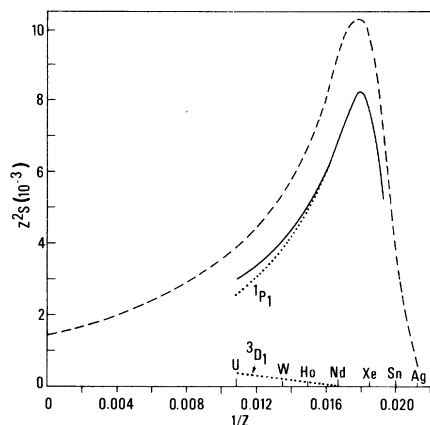


FIG. 8. Comparison of the unperturbed Hartree-Fock  $4d^{10}1S-4d^94f^1P$  line strength (dashed), the results of a limited perturbation-theory calculation (solid), and an intermediate-coupling calculation involving the  $4d^94f^3P_1$ ,  $^3D_1$ ,  $^2P_1$ , and  $4d^95p^3P_1$ ,  $^3D_1$ , and  $^1P_1$  states (dotted).

should be much smaller than correlation effects since the large angular momentum of the optical electrons precludes substantial probability density close to the nucleus. Deviations from LS coupling are small, as may be seen in Fig. 8, which compares the term-dependent Hartree-Fock line strength with the results of an intermediate-coupling calculation involving the  $4d^94f^3P_1$ ,  $^3D_1$ , and  $4d^95p^3P_1$ ,  $^1P_1$ ,  $^3D_1$  levels.

At present there are no experimental data available for the oscillator strengths of Pd-like ions. This is primarily a result of the short lifetimes involved ( $\sim 10^{-12}$  sec) and the difficulty in generating such heavy highly ionized species in quantities large enough to be useful in a lifetime experiment. It is hoped that the present calculations will provide an incentive for further experimental investigations of the radiative data of highly ionized heavy atoms.

#### ACKNOWLEDGMENT

This work was supported in part by the Department of Energy, Office of Magnetic Fusion Energy.

<sup>1</sup>W. L. Wiese, in *Progress in Atomic Spectroscopy*, edited by W. Hanle and H. Kleinpoppen (Plenum, New York, 1979), part B.

<sup>2</sup>C. F. Fischer, *J. Phys. B* **7**, 1241 (1977).

<sup>3</sup>S. M. Younger, *Phys. Rev. A* **20**, 951 (1979).

<sup>4</sup>C. F. Fischer and J. E. Hansen, *Phys. Rev. A* **17**, 1956 (1978).

<sup>5</sup>D. Shorer, *Phys. Rev. A* **18**, 1060 (1978).

<sup>6</sup>A. W. Weiss (private communication).

<sup>7</sup>S. M. Younger and W. L. Wiese, *Phys. Rev. A* **17**, 1944 (1978).

<sup>8</sup>K. Cheng and Y. K. Kim, *J. Opt. Soc. Am.* **69**, 125 (1979).

<sup>9</sup>S. M. Younger and A. W. Weiss, *J. Res. Nat. Bur. Stds.*

- (U.S.) 79A, 629 (1975).
- <sup>10</sup>C. F. Fischer, *The Hartree-Fock Method for Atoms* (Wiley, New York, 1977).
- <sup>11</sup>J. Slater, *Quantum Theory of Atomic Structure* (McGraw-Hill, New York, 1960), Vol. II.
- <sup>12</sup>J. Sugar, *J. Opt. Soc. Am.* 67, 1518 (1977).
- <sup>13</sup>M. Even-Zohar and B. S. Fraenkel, *J. Phys. B* 5, 1596 (1972).
- <sup>14</sup>H. P. Kelly, in *Atomic Inner Shell Processes*, edited by B. Crasemann (Academic, New York, 1975).
- <sup>15</sup>S. M. Younger, *Phys. Rev. A* 21, 1364 (1980).